REVISITING THE ASSUMPTION OF LATENT SEPARABILITY FOR BACKDOOR DEFENSES

Anonymous authors
Paper under double-blind review

ABSTRACT

Recent studies revealed that deep learning is susceptible to backdoor poisoning attacks. An adversary can embed a hidden backdoor into a model to manipulate its predictions by only modifying a few training data, *without controlling the training process*. Currently, a tangible signature has been widely observed across a diverse set of backdoor poisoning attacks — models trained on a poisoned dataset tend to learn separable latent representations for poison and clean samples. This latent separation is so pervasive that a family of backdoor defenses directly take it as a default assumption (dubbed *latent separability assumption*), based on which to identify poison samples via cluster analysis in the latent space. An intriguing question consequently follows: *is the latent separation unavoidable for backdoor poisoning attacks*? This question is central to understanding whether the assumption of latent separability provides a reliable foundation for defending against backdoor poisoning attacks. In this paper, we design *adaptive backdoor poisoning attacks* to present counter-examples against this assumption. Our methods include two key components: (1) a set of trigger-planted samples correctly labeled to their semantic classes (other than the target class) that can regularize backdoor learning; (2) asymmetric trigger planting strategies that help to boost attack success rate (ASR) as well as to diversify latent representations of poison samples. Extensive experiments on benchmark datasets verify the effectiveness of our adaptive attacks in bypassing existing latent separation based backdoor defenses. Moreover, our attacks still maintain a high attack success rate with negligible clean accuracy drop. Our studies call for defense designers to take caution when leveraging latent separation as an assumption in their defenses.

1 INTRODUCTION

Overparameterized deep neural network (DNN) models can fit complex datasets perfectly and generalize well on i.i.d. data distributions. However, the strong expressivity of these models also render them susceptible to *backdoor poisoning attacks* (Gu et al., 2017; Chen et al., 2017; Turner et al., 2019; Li et al., 2022). In a backdoor poisoning attack, an adversary only manipulates a small portion of the victim's training dataset. The victims will train their own model on the manipulated dataset and consequently get a backdoored model. Typically, the adversary will *poison* the victim's dataset by injecting a small amount of backdoor poison samples, each of which contains a backdoor trigger (e.g. a specific pixel patch) and is labeled to a specific target class. A DNN model trained on this poisoned dataset will be backdoored in that they tend to learn an artificial correlation between the backdoor trigger and the target class. These attacks are stealthy since backdoored models behave normally on natural samples and therefore users can hardly identify them.

Despite the stealthiness in terms of model performance on natural samples, it has been commonly observed (Tran et al., 2018; Chen et al., 2018; Huang et al., 2022) that backdoor poisoning attacks tend to leave tangible signatures in the latent space of backdoored models. As visualized in Fig 1b - Fig 1g, poison and clean samples from the target class consistently form two separate clusters in the latent space, across a diverse set of backdoor poisoning attacks. The pervasiveness of the latent separation renders itself oftentimes as a default assumption, which we call *latent separability assumption* in this work. A family of defenses (i.e., *latent separation based backdoor defenses*) explicitly base their designs on this assumption. These defenses first train a base classifier on the poisoned dataset, and expect the base model will naturally learn separable latent representations

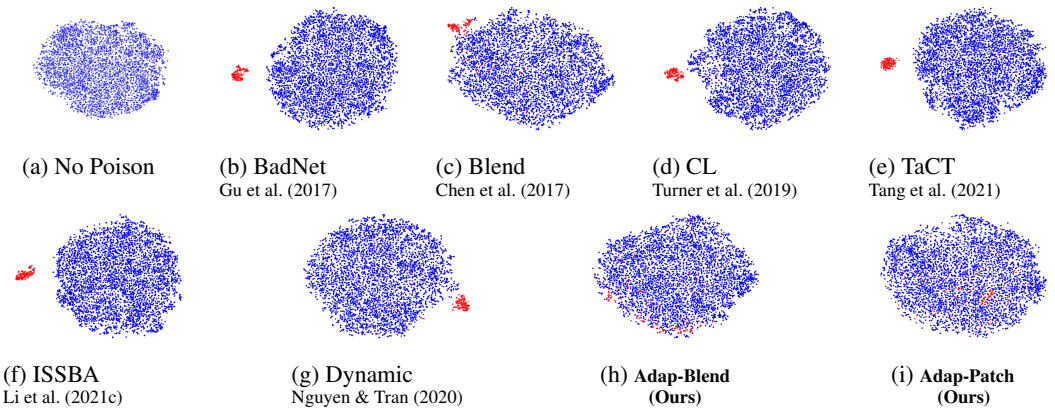

Figure 1: T-SNE visualization of latent separability characteristic on CIFAR-10. Each point in the plots corresponds to a training sample from the target class. Caption of each subplot specifies its corresponding poison strategy. To highlight the separation, all poison samples are denoted by red points, while clean samples correspond to blue points.

for poison and clean samples respectively. After that, they perform cluster analysis on the latent space of the base model. If the latent separation characteristics reliably arise, these defenses will be able to identify the outlier cluster formed by poison samples, and thus accurately filter out these poison samples from the training set. We note that *this family of defenses are particularly important and successful in the backdoor defense literature*. Popular proposals in this family like Spectral Signature (Tran et al., 2018) and Activation Clustering (Chen et al., 2018) have already become indispensable baselines, and recent state-of-the-art proposals including SCAn (Tang et al., 2021) and SPECTRE (Hayase et al., 2021) in this family even claim to achieve nearly perfect recall with negligible false positive rate against a diverse set of attacks. Given the pervasiveness of the latent separation and its profound success in the application of backdoor defenses, a natural question arises: ***Is the latent separation unavoidable for backdoor poisoning attacks?***

In this work, we revisit the assumption of latent separability and expose failure regions of defenses based on it. Specifically, we design adaptive backdoor poisoning attacks (without control of the model training process), which can actively suppress the latent separation while maintaining a high attack success rate (ASR) with negligible clean accuracy drop. Two critical components are underlying the design of our adaptive attacks (see Fig 2 for an overview): (1) *Data poisoning based regularization*. After planting the backdoor trigger to a set of samples, we do not mislabel all of them to the target class. Instead, we randomly keep a fraction of them (namely regularization samples) still correctly labeled to their real semantic classes. Intuitively, these additional regularization samples penalize the backdoor correlation between the trigger and the target class. (2) *Trigger planting strategies that promote asymmetry and diversity.* One may notice that penalization on the backdoor correlation induced by regularization samples can also greatly hurt the attack success rate (ASR). We alleviate this problem via asymmetric trigger planting strategies. As illustrated in Fig 2, we apply weakened triggers when we construct regularization and payload samples for data poisoning, while the original standard trigger would only be used during test time to activate the backdoor. Conceptually, in this way, since test-time backdoor samples (with the standard trigger) contain stronger backdoor features than those of regularization samples (with weakened triggers), the test-time attack can well mitigate the counter force from regularization samples and still maintain a high ASR. Beside asymmetry, our design also promotes diversity of triggers during data poisoning — different poison samples could be stamped with different partial triggers, selected from a diverse set of trigger partitions. Intuitively, this diversity allows backdoor poison samples to scatter more diversely in the latent representation space, and can thus avoid being aggregated into an easy-to-identify cluster.

In conclusion, the main contributions of this paper are four-fold. **(1)** We confirm that the latent separability assumption holds across a diverse set of backdoor poisoning attacks in the existing literature. **(2)** We reveal that this assumption could fail, leading to poor performance of defenses that explicitly base their designs on it. **(3)** We design some simple yet effective adaptive backdoor poisoning attacks to present counter-examples against this assumption with two key novel components. **(4)** We conduct extensive experiments on benchmark datasets, verifying the effectiveness and the stealthiness in countering detection methods of our adaptive attacks.

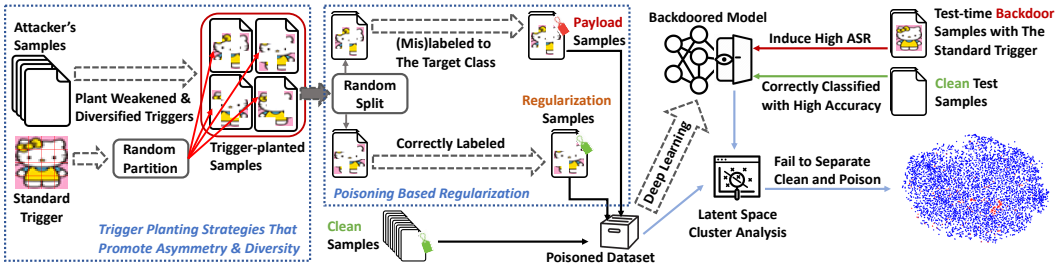

Figure 2: An overview of our adaptive backdoor poisoning attacks (here we take Adaptive-Blend introduced in Sec 5.2 as an example for illustration). Two key components render our attacks adaptive: (1) Poisoning based regularization, which penalizes the backdoor correlation and helps to suppress the latent separation; (2) Trigger planting strategies that promote asymmetry and diversity, which help to maintain a high attack success rate as well as to improve latent space stealthiness. Please refer to our Section 5.1 for more technical details.

2 Related Work

Backdoor Poisoning Attacks. Backdoor poisoning attacks (Gu et al., 2017; Chen et al., 2017; Turner et al., 2019; Li et al., 2021c) are also frequently referred to as poison-only backdoor attacks. This category of attacks only assume control over a small portion of the victim's training data, while the victim will train her own models on the poisoned dataset from scratch. Other backdoor attacks that assume additional control over the training process (Shokri et al., 2020) or even weights of deployed models (Liu et al., 2017a; Qi et al., 2022) do not fall in this category and are not considered in this work. We refer interested readers to Li et al. (2022) for a more comprehensive review.

Latent Separation for Backdoor Defenses. It has been commonly observed (Tran et al., 2018) that models trained on a poisoned dataset tend to learn very different latent representations for backdoor and clean samples in the target class, which form two separate clusters (see Fig 1). This phenomenons is so pervasive that a family of defenses directly take the latent separation as a default assumption and propose to identify poison samples via performing cluster analysis on the latent space. This family includes Spectral Signature (Tran et al., 2018) and Activation Clustering (Chen et al., 2018), which are most commonly evaluated baselines. More recent proposals (Tang et al., 2021; Hayase et al., 2021) in this family further claim to achieve nearly perfect recall with negligible false positive rate against a diverse set of attacks even in very low poison rate cases.

Adaptive Backdoor Attacks Against Latent Separation Based Defenses. A family of adaptive backdoor attacks (Shokri et al., 2020; Xia et al., 2021; Doan et al., 2021; Ren et al., 2021; Cheng et al., 2020; Zhong et al., 2022) explicitly aim to reduce the latent separation between poison and clean samples. However, they do not fit into the paradigm of backdoor poisoning attacks — they assume additional control over the whole training process and thus directly encode the latent inseparability into the training objectives of attacked models. A more relevant work is Tang et al. (2021), which points out that their source-specific poison-only attack can reduce latent separation. However, as shown in Fig 1e, when the base model is trained along with standard data augmentation, *there is still a notable separation* between the clean and poison populations, and actually Tang et al. (2021) themselves also show that an improved latent space cluster analysis suffices to perfectly separate poison and clean samples of this attack. *Thus, it is still unclear whether a poison-only backdoor attack can overcome the latent separation to evade backdoor defenses built on it.* In this work, we fill the gap and design adaptive backdoor poisoning attacks that can actively suppress the latent separation (and thus circumvent existing latent separation based defenses).

Other Backdoor Defenses. There are some other defenses that are not built on the latent separation. These include trigger synthesis (Wang et al., 2019), model diagnosis (Xu et al., 2021; Kolouri et al., 2020), fine-tuning based approaches (Liu et al., 2017b; Li et al., 2021b), and poison suppression (Du et al., 2019; Li et al., 2021a), etc. Most of these proposals also have their own limitations revealed by existing literature (refer Li et al. (2022)), but they are not our focus in this work.

3 NOTATIONS AND THREAT MODEL

Notations. We study image classification with DNN models. We denote a model by $\mathcal{F}_\theta : \mathcal{X} \mapsto [C]$, where θ are trainable parameters, $\mathcal{X}$ is the input space, C is the number of classes, and $[C] := \{1, 2, \ldots, C\}$. We decompose $\mathcal{F}_\theta$ as $\mathcal{F}_\theta = l_\theta \circ f_\theta$, where l_θ is the last linear prediction layer that transforms a latent representation into the final prediction label, and f_θ is the feature extractor. Given an input $x \in \mathcal{X}$, $f_\theta(x) \in \mathcal{H}$ is the latent representation of x w.r.t model $\mathcal{F}_\theta$, $\mathcal{H}$ denotes the latent representation space, and $\mathcal{F}_\theta(x) = l_\theta \circ f_\theta(x)$ is the predicted label. For backdoor poisoning attacks, we denote the clean training set by $\mathcal{D} = \{(x_i, y_i) \mid i = 1, \ldots, n\}$. We denote the backdoor trigger planting strategy by a transformation $\mathcal{T} : \mathcal{X} \mapsto \mathcal{X}$, and the adversary's poison label flipping strategy is denoted by $\mathcal{L} : \mathcal{X} \times [C] \mapsto [C]$. We use $\mathcal{J} := \{j_1, \ldots, j_p\}$ to denote indices of the p data points that are controlled by the adversary. The resulting poisoned training set is denoted as $\mathcal{D}_{\text{poison}} = \{(\tilde{x}_i, \tilde{y}_i) \mid i = 1, \ldots, n\}$, where

$$\tilde{x}_i = \begin{cases} \mathcal{T}(x_i), & i \in \mathcal{J} \\ x_i, & \text{otherwise} \end{cases}, \qquad \tilde{y}_i = \begin{cases} \mathcal{L}(x_i, y_i), & i \in \mathcal{J} \\ y_i, & \text{otherwise} \end{cases}. \tag{1}$$

Threat Model. We consider the standard threat model of backdoor poisoning attacks (poison-only backdoor attacks), where the adversary *only* control a small portion of the victim's training data and the victim will *train her own models from scratch* on the poisoned dataset manipulated by the adversary. Specifically, the adversary will design a trigger planting strategy $\mathcal{T}$ and a label flipping strategy $\mathcal{L}$ to manipulate the controlled p training samples (as formulated in Eqn 1). A victim model trained on the poisoned dataset $\mathcal{D}_{\text{poison}}$ will be backdoored — that is, during test time, the model will (mis)classify a trigger-planted input to a target class t with high probability, while keep approximately the same performance to that of a benign model on genuine inputs.

4 PROBLEM FORMULATION: TOWARDS POISON-ONLY BACKDOOR ATTACKS THAT CAN ACTIVELY SUPPRESS THE LATENT SEPARATION

Latent Separability Assumption for Backdoor Defense. Given a poisoned dataset $\mathcal{D}_{\text{poison}}$, one can train a backdoored model $\mathcal{F}_\theta := l_\theta \circ f_\theta$ via running a standard empirical risk minimization procedure h on $\mathcal{D}_{\text{poison}}$, i.e. $\theta \in h(\mathcal{D}_{\text{poison}})$. Latent separability assumption indicates that, in the latent representation space generated by the backdoored model $\mathcal{F}_\theta$, poison and clean samples from the target class t will form separate clusters, while samples from a non-target class only form a single homogeneous cluster (see Fig 1). Latent separation based backdoor defenses (Tran et al., 2018; Chen et al., 2018; Hayase et al., 2021; Tang et al., 2021) propose to run cluster analysis on $H^c = \{f_\theta(\tilde{x}_i) | \tilde{y}_i = c\}$ for each class c. Typically, the defender will design a heterogeneous criterion $\mathcal{I}(\cdot)$ that takes H^c as input and judges whether this set is heterogeneous (i.e. contains separate clusters). On the heterogeneous H^t identified by the criterion $\mathcal{I}$, the cluster analysis will divide H^t into two empirical clusters H^t_B and H^t_A, where H^t_A is the suspected cluster formed by poison samples. The dataset will be cleansed by simply removing those training samples that generate H^t_A.

Our Goals. This work revisits the assumption of latent separability for backdoor defenses against poison-only backdoor attacks. We investigate *adaptive backdoor poisoning attacks* that can actively suppress the latent separation between poison and clean samples. Ideally, against such adaptive attacks, the criterion $\mathcal{I}$ used by a defense should fail to detect the heterogeneity in H^t and the cluster analysis would neither accurately separate poison and clean samples.

Perspectives that Motivate Our Design. Two heuristic and mutually complementary perspectives on the latent separation phenomenon have inspired our design in this work. The <u>first</u> perspective attributes the latent separation to *the dominant impact of backdoor triggers* (Tran et al., 2018) during the inference of backdoored models. The intuition is — in order to "push" a (trigger-planted) backdoor poison sample from its semantic class to the target class, a backdoored model tends to learn an excessively strong signal for the backdoor trigger pattern in latent representation space such that the signal can overwhelmingly beat other semantic features to make its dictatorial decision. The strong backdoor signal that exclusively appears in backdoor poison samples thus leads to the separation. The <u>second</u> perspective is that, backdoored models learn separate representations for poison and clean samples simply because they tend to *learn a separate shortcut rule* (Geirhos et al., 2020) (solely based on the trigger pattern) to fit those poison samples without using any semantic features. The sense is — backdoor learning is often independent of (or only weakly correlated to) the semantic features used by the main task, thus the backdoored model that fits the poisoned dataset essentially just learns two unrelated (or weakly related) tasks. From this aspect, there is not even an

appealing reason for backdoor models to learn homogeneous latent representations for samples from the two heterogeneous tasks. Motivated by these perspectives, we conceive that a desirable adaptive backdoor poisoning attack (that can mitigate the latent separation) might need to encode some form of regularization, so as to (1) penalize the backdoored model for learning abnormally strong signals for the backdoor trigger; (2) encourage interconnection between backdoor learning and learning of the main task. These intuitions finally lead to our design in Sec 5.

5 Our Methods

We design *adaptive* backdoor poisoning attacks following the insights we introduce in Sec 4. In Sec 5.1, we first present the generic framework underlying the design of our attacks. Then, in Sec 5.2, we elaborate concrete attacks that we implement in this work.

5.1 A Generic Framework for Adaptive Backdoor Poisoning Attacks

Overview. We present an overview of our design in Fig 2. Unlike typical backdoor poisoning attacks, in our framework, we do not label all trigger-planted samples to the target class. As shown, after planting the backdoor trigger to a set of samples (sampled from all classes), we randomly split them into two disjoint groups. For one group, we still label them to the target class (we call this group *payload samples*) to establish the backdoor correlation between the trigger pattern and the target label; while the other group (namely *regularization samples*) will instead be correctly labeled to their real semantic classes (that can be diffident from the target class) to regularize the backdoor correlation. Formally, following our notations in Sec 3, the adversary will specify a *conservatism ratio* $\eta \in [0, 1)$, with which our label flipping strategy formulates as:

$$\mathcal{L}(x_i, y_i) = \begin{cases} t, & \text{with probability } 1 - \eta \\ y_i, & \text{with probability } \eta \end{cases} . \tag{2}$$

Moreover, we introduce ideas of asymmetry and diversity into our trigger design — we apply a diverse set of weakened triggers to construct regularization and payload samples for data poisoning, while the original standard trigger is used during test time to activate the backdoor.

Regularization Samples. We note that, *the introduction of regularization samples well incorporates our two insights from Sec 4.* First, with regularization samples, the backdoored model can no longer learn a dominantly strong signal for the backdoor trigger that dictatorially votes for the target class, otherwise, it can not fit regularization samples that are correctly labeled to other classes. This explains the naming of *regularization samples* — intuitively, they serve as regularizers that help to penalize the backdoor signal in the learned latent representations. Second, the model can neither fit all trigger-planted samples via a simple shortcut rule. Instead, now *it has to fit a much more complicated boundary* that should decide when to classify a trigger-planted input to the target class and when to classify it to its real semantic label, where the boundary is randomly generated. To successfully fit this boundary, the model must rely on both the trigger pattern and artifacts from the semantic features that coexist with the trigger, thus the learned latent representations for backdoor samples should be a more balanced fusion of both the trigger pattern and semantic features.

Asymmetric Triggers. *The introduction of asymmetric triggers is critical for our attacks to still maintain a high attack success rate (ASR).* As one may easily notice, since regularization samples penalize the backdoor correlation, a side-effect could be the drop of attack success rate (ASR). To mitigate this problem, rather than using the same trigger for both data poisoning and test-time attack, in our design, we apply weakened triggers for data poisoning and use the (stronger) original standard trigger only for the test time. The intuition is: During test time, the backdoor samples (with the standard trigger) contain stronger backdoor features than those of regularization samples (with weakened triggers). This then enables test-time backdoor samples to have sufficient "power" to mitigate the counter force from regularization samples and thus to still achieve a high ASR. We note that the idea of asymmetric triggers traces earliest back to Chen et al. (2017), however the context is different. In order to evade human inspection on the poisoned dataset, Chen et al. (2017) propose to use weakened triggers that are visually less evident for data poisoning, and point out that a high ASR can still be maintained if the original standard trigger is used in test time. In our context, we use weakened triggers mainly to undermine the negative impact induced by regularization samples.

Trigger Diversification. We also highlight that *the trigger diversification in our design can also help our attacks to mitigate the latent separation.* Intuitively, since different poison samples could be planted with different triggers, these poison samples may scatter more diversely in the latent

representation space. We expect such a more diverse scattering can prevent these poison samples from aggregating into an easy-to-identify cluster.

5.2 Instantiations of Our Attacks

Note that, our framework presented in Fig 2 is generic and can be creatively combined with existing techniques to instantiate powerful adaptive attacks. Following this framework, we instantiate two concrete attacks via directly adapting commonly used image blending based and patch based poison strategies, namely *Adaptive-Blend* and *Adaptive-Patch* respectively.

Figure 3: In Adaptive-Blend, we partition the full trigger image into $4 \times 4 = 16$ pieces (left), and randomly apply only 50% of these trigger pieces (right) to each poison sample, during data poisoning. Red lines demonstrate the grids by which we randomly mask the original trigger.

Adaptive-Blend. An interesting point revealed by Fig 1 is that the simple Blend attack (Chen et al., 2017) turns out to induce the least latent separation, better than many attacks that are usually deemed more advanced and stealthy. This suggests image blending based triggers as good candidates for designing attacks with weak latent separation. For this reason, we design *Adaptive-Blend* via directly adapting the naive Blend attack according to our framework. Specifically, Adaptive-Blend introduces a conservatism ratio of $\eta = 0.5$ to balance the number of payload and regularization samples, and still adopts the process $\tilde{x} = (1 - \alpha) * x + \alpha * T$ from Chen et al. (2017) to blend the trigger pattern T into a genuine image x to construct the trigger-planted sample $\tilde{x}$. As for asymmetric design, we still take the standard $\alpha = 0.2$ for test-time attacking, but use a weaker asymmetric opacity of $\alpha = 0.15$ for poison samples. Moreover, for a stronger and more diverse asymmetry, we propose to partition the standard full trigger (Fig 3, left) into $4 \times 4 = 16$ pieces — the full trigger would still be used for test-time attacking, while we randomly apply only 50% of the partitioned trigger pieces (e.g. Fig 3, right) to each poison sample during data poisoning. This additional partition boosts both the ASR and the latent space stealthiness (see Sec 6.3.3).

Adaptive-Patch. Although the triggers could be more visually detectable, for comprehensiveness, we also instantiate our adaptive attack with patch based triggers, namely Adaptive-Patch. Empirically, since patch based triggers usually induce stronger latent separation (e.g. see Fig 1b), we correspondingly turn to a larger conservatism ratio of $\eta = 2/3$. For trigger planting, rather than sticking to a single patch pattern, we prepare a more diverse set of 4 patch triggers (Fig 6c-6f) for data poisoning. Specifically, each poison sample is randomly attached to only one of the four triggers with a low opacity (e.g., 50%) (Fig 6j-6m). At test time, we asymmetrically apply two (of the four) fully opaque triggers (e.g., Fig 6g) simultaneously to achieve high ASR.

6 Experiments

6.1 Setup

Datasets and Model Architectures. We evaluate our adaptive attacks on three benchmark datasets that are commonly used in backdoor learning literature: CIFAR-10 (Krizhevsky, 2012), GTSRB (Stallkamp et al., 2012) and a 10-classes subset of Imagenet (Russakovsky et al., 2015). For building base models, we also consider three different architectures including ResNet-20 (He et al., 2016), VGG-16 (Simonyan & Zisserman, 2014) and Mobilenet-V2 (Sandler et al., 2018). Due to the space limit, in this section, we only present our results on CIFAR-10 with ResNet-20. We refer interested readers to Appendix B for results on other datasets and architectures. Detailed configurations on dataset split and training details of base models are deferred to Appendix A.

Attacks. We evaluate our `Adap-Blend` and `Adap-Patch` attacks presented in Section 5.2. Besides, we also compare our adaptive attacks with six representative attacks in the literature. These attacks correspond to a diverse set of poisoning strategies including both classical and advanced ones. `BadNet` (Gu et al., 2017) and `Blend` (Chen et al., 2017) correspond to typical dirty-label attacks with patch-like triggers and blending based triggers respectively. `Dynamic` (Nguyen & Tran, 2020) and `ISSBA` (Li et al., 2021c) correspond to input-aware backdoor attacks. `CL` (Turner et al., 2019) is a clean label attack. `TaCT` (Tang et al., 2021) is a source-specific attack. Unless explicitly specified, for every attack, by default, we use 150 (payload) poison samples for data poisoning. Detailed attack configurations are described in Appendix A.2.

Table 1: Latent separability based defenses against our adaptive attacks on CIFAR-10.

	(%)	No Poison	Blend	BadNet	ISSBA	Dynamic	CL	TaCT	**Adap-Blend (Ours)**	**Adap-Patch (Ours)**
Without Defense	ASR	/	89.0	99.9	95.3	97.5	93.6	96.5	76.5	97.5
	Clean Accuracy	92.0	91.7	91.5	91.6	91.8	92.1	91.8	91.6	91.5
Spectral Signature Tran et al. (2018)	Elimination Rate	/	53.8	98.0	63.5	87.8	94.4	62.9	13.3	10.0
	Sacrifice Rate	15.0	4.4	4.2	4.3	4.3	4.2	4.3	4.5	4.5
	ASR	/	58.6	1.3	1.1	72.4	40.8	96.4	62.0	93.1
	Clean Accuracy	90.9	91.5	91.4	91.5	86.1	91.7	91.6	91.5	91.5
Activation Clustering Chen et al. (2018)	Elimination Rate	/	0.0	100.0	0.0	30.6	33.3	33.1	0.0	0.0
	Sacrifice Rate	0.0	0.0	7.1	0.0	5.3	1.0	5.4	0.0	0.0
	ASR	/	87.8	1.1	95.3	69.7	62.2	65.2	76.0	97.5
	Clean Accuracy	92.0	91.7	91.4	91.6	91.5	92.1	91.6	91.6	91.5
SCAn Tang et al. (2021)	Elimination Rate	/	0.0	99.1	91.8	62.9	66.7	100.0	0.0	0.0
	Sacrifice Rate	0.0	0.0	3.5	0.9	0.0	4.0	4.9	1.2	0.0
	ASR	/	87.8	1.0	0.9	46.3	32.9	28.0	78.2	97.5
	Clean Accuracy	92.0	91.7	91.1	91.6	91.7	91.8	90.8	91.6	91.5
SPECTRE Hayase et al. (2021)	Elimination Rate	/	96.4	100.0	100.0	99.8	100.0	100.0	6.9	0.0
	Sacrifice Rate	1.5	0.2	0.2	0.2	0.2	0.2	0.2	0.5	0.5
	ASR	/	5.7	0.8	1.0	7.7	1.6	1.7	69.0	94.8
	Clean Accuracy	91.6	91.7	91.7	91.6	91.6	91.6	91.6	91.4	91.6
Silhouette Score		/	0.2608	0.4744	0.3933	0.4358	0.3964	0.2866	**0.1065**	**0.0856**

Defenses. To validate the "adaptiveness" of our attacks against latent separation based backdoor defenses, we evaluate the four state-of-the-art defenses from this family: Spectral Signature (Tran et al., 2018), Activation Clustering (Chen et al., 2018), SCAn (Tang et al., 2021) and SPECTRE (Hayase et al., 2021). All of these defenses are designed to detect and eliminate backdoor poison samples from the poisoned dataset, based on the assumed latent separation characteristics.

Metrics. For backdoor defenses that we evaluate, we measure their: 1) *Elimination Rate*, ratio of (payload) poison samples that they successfully detect; 2) *Sacrifice Rate*, ratio of clean samples falsely eliminated; 3) *Attack Success Rate (ASR)* of models retrained on the cleansed set; 4) *Clean Accuracy* of models retrained on the cleansed set. Note that, ASR is the standard metric defined as the ratio of trigger-planted samples that are mispredicted to the target class, while clean accuracy is the standard accuracy on genuine test samples. Moreover, to quantify the latent separation between clean and poison samples, we report the *Silhouette Score* (Rousseeuw, 1987) for clean and poison representations in the target class. A silhouette score is in the range from 0 to 1. A lower silhouette score indicates weaker separation. All the numbers that we report are average results across three independent repeated experiments.

6.2 Attack Results

Visualization. Figure 1 plots latent representations of poison and clean samples for different attacks, visualized by T-SNE (Van der Maaten & Hinton, 2008). As shown, notable latent separations are consistently observed on all the baseline attacks that we consider, while the poison and clean samples of our attacks mix with each other (Fig 1h,1i). To further reveal the extent of latent inseparability of our adaptive attacks, we also use Support Vector Machine (SVM (Cortes & Vapnik, 1995)) to find the (linear) boundary that best separates poison and clean samples in the latent representation space. Fig 4 visualizes the histogram of distances between each data point and the SVM hyperplane. As shown, compared to non-adaptive attacks (Fig 4a and 4c), our adaptive attacks (Fig 4b and 4d) bring the poison and clean samples much closer.

Against Latent Separation Based Defenses. We present our main results in Table 1. As shown, against SPECTRE (Hayase et al., 2021) defense, the strongest latent separation based defense in the literature, none of the six baseline attacks survive — SPECTRE can always eliminate almost all poison samples with negligible sacrifice of clean samples. This is consistent with our (qualitative) visualization in Fig 1, where notable latent separations are observed for all these attacks. It is also consistent with our quantitative measure of the latent separation — all the six baseline attacks induce high Silhouette scores (> 0.25). In comparison, our two adaptive attacks exhibit evident stealthiness in the latent representation space — both the visualization results (Fig 1h,1i) and Silhouette scores indicate much weaker latent separation, and all the four latent separation based defenses are consistently defeated (ASR is still larger than 20% after defense). Besides, our adaptive attacks always achieve high ASR with negligible clean accuracy drop in all the cases. When no defense is applied, both Adap-Blend (>75%) and Adap-Patch achieve high ASR (>95%). While none of the other six baseline attacks makes thorough all these defenses after cleansing and retraining, both our Adap-Blend and Adap-Patch consistently retain considerable ASR (Adap-Blend $> 60\%$ and Adap-Patch $> 90\%$), surviving each of them. We point out that, our results serve as clear counter

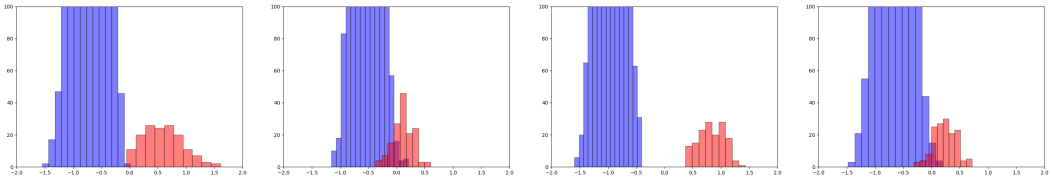

(a) Blend (b) Adap-Blend (c) BadNet (d) Adap-Patch

Figure 4: Visualization of latent representation spaces fitted by SVM. We use SVM to find the optimal (linear) boundary that separates poison and clean samples, and plot the histograms of (signed) distances between each point and the SVM hyperplane.

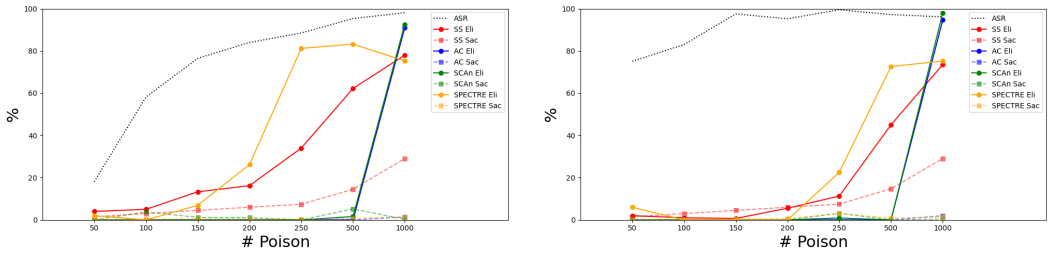

(a) Adap-Blend (b) Adap-Patch

Figure 5: Defense results w.r.t. different (payload) poison samples. For Adap-Blend, we use as many regularization samples as payload samples; for Adap-Patch, we use twice the regularization sample number as payload samples. The black dotted lines show the ASR. We use different colors to represent the results of different defenses, where the solid lines correspond to Elimination ("Eli") and the dotted lines correspond to Sacrifice ("Sac").

Table 2: Adap-Blend with different regularization sample numbers, with fixed 150 payload samples.

(%)	# Regularization Samples	0	50	100	150	200	250	300	350	400	450
	ASR	89.0	86.5	83.9	76.5	74.1	70.4	65.6	60.9	58.0	56.5
SPECTRE	Elimination Rate	67.3	45.3	37.1	6.9	0.0	0.0	0.0	0.0	0.0	0.0
	Sacrifice Rate	0.2	0.3	0.3	0.5	0.5	0.5	0.5	0.5	0.5	0.5
	ASR	9.1	29.2	37.9	69.0	78.2	68.5	57.9	68.7	64.0	62.8

examples against the assumption of latent separability and the "adaptiveness" of our attacks are also validated. We also note that, similar results also hold on other datasets and model architectures (see Appendix B).

6.3 Ablation Studies

6.3.1 Poison Rate

As mentioned in Sec 6.1, our main experiments consistently use 150 (payload) poison samples for poisoning attack. In Fig 5, we supplement additional results of our adaptive attacks with different number of poison samples. Specifically, we increase the number of payload poison samples from 50 to 1000, and the number of regularization samples also proportionally vary according to the fixed conservatism ratio η that we specify in Sec 5.2. As shown, one key takeaway is — when the poison sample number grows too large (e.g., 1000), the stealthiness of our adaptive attacks start to significantly degrade. This is not surprising — with more and more poison samples containing the rigid trigger pattern, the trigger pattern would become increasingly statistical significant, and models will unavoidably learn strong signal for this pattern in spite of the regularization. This indicates that a moderate poison rate is also a necessary condition for the success of our adaptive attacks.

6.3.2 Strength of Regularization

Now, we fix the number of payload poison samples (150 samples), and investigate varying number of regularization samples — this reflects different strength of regularization. Specifically, we evaluate

Adap-Blend against SPECTRE, and present the results in Tab 2. We can generally tell that: 1) when the regularization is weak (e.g. 0, 50, 100 regularization samples), our adaptive attacks could still be detected; 2) when the regularization is becoming stronger, our adaptive attacks start to mitigate the defense, though the ASR suffers from more sacrifice.

6.3.3 Is every part of our adaptive strategy necessary?

Table 3: Ablation study to see if every part of our adaptive strategy is necessary.

(a) Blending attack with lower poison rates.

(%)	ASR	SPECTRE	
# Poison Samples		Elimination	Retrained ASR
50	69.7	84.0	8.7
100	81.4	97.0	5.3
150	89.0	96.4	5.7

(b) Adap-Blend with partial components.

(%)	ASR	SPECTRE	
		Elimination	Retrained ASR
No Diversity & Asymmetry	52.1	28.0	32.5
No Regularization Samples	89.0	67.3	9.1
With Both	76.5	6.9	69.0

Simply reducing poison rate is not enough. In Sec 6.3.1, we real that a low poison rate is necessary for the success of our attacks. Nonetheless, as shown in Tab 3a, when we lower the poison rate of blending attack, it will still be cleansed by SPECTRE (even when there are as few as 50 poison samples). Thus, simply reducing poison rate is not sufficient for mitigating the latent separation.

Simply relying on regularization samples is not enough. Regularization samples are important in our design, so is the trigger planting strategy we adopted (See Sec 5.1 for discussion). If we use the standard symmetric trigger for both the data poisoning and test-time attack, both the ASR and latent space stealthiness would degrade — the first row of Tab 3b shows Adap-Blend without asymmetric trigger partitioning, where it has a lower ASR ($\approx 50\%$) and could be further suppressed (retrained ASR $\approx 30\%$) by SPECTRE.

Simply relying on asymmetric and diversified triggers is not enough. Reversely, we study how our adaptive strategy behaves when we don't use regularization sample and rely solely on our trigger planting strategy. As shown in the second row of Tab 3b, though the original ASR gets higher, as a trade off, a much larger fraction ($> 67\%$) of the poison samples can now be recognized and removed by SPECTRE and the retrained ASR drops severely. This further confirms that regularization samples are vital for the success of our attacks.

7 Discussions

Ideally, we hope a perfect adaptive attack can make the poison and clean samples completely indistinguishable. This has been achieved under stronger threat model when the the training process is also controlled Shokri et al. (2020); Xia et al. (2021); Doan et al. (2021); Ren et al. (2021); Cheng et al. (2020); Zhong et al. (2022). In this paper, we take a step further to this goal under poisoning-only threat model. We successfully come up with adaptive backdoor poisoning attacks that can suppress the latent separability and circumvent existing defenses based on latent separability. However, as shown in Fig 4, under oracle visualization, there is still a difference between poison and clean distributions, though the difference is greatly reduced. A key remaining question is — is it possible to achieve the ideal indistinguishable goals with poison-only adversary? We encourage future work to look into this question. Besides, since we introduced attacks that may not be defended by many existing techniques, we note that this exposes existing systems built on these defenses to risks. We encourage future work on designing stronger defenses that resist our attacks.

8 Conclusion

In this work, we revisit the assumption of latent separability for backdoor defenses. We reveal that this assumption could fail, leading to failure of backdoor defenses built on this assumption. Specifically, we provide our insights on the phenomenon of latent separation, and design adaptive attacks that can mitigate this separation. Empirical study and evaluation on various latent separation based defenses show that our adaptive poisoning attacks indeed suppress the latent separation and render them ineffective. We call for every defense designer to take caution when leveraging the latent separability as an assumption in their defenses. We also encourage further defenses to take our attacks into consideration for a more comprehensive evaluation.

REFERENCES

Bryant Chen, Wilka Carvalho, Nathalie Baracaldo, Heiko Ludwig, Benjamin Edwards, Taesung Lee, Ian Molloy, and Biplav Srivastava. Detecting backdoor attacks on deep neural networks by activation clustering. *arXiv preprint arXiv:1811.03728*, 2018.

Xinyun Chen, Chang Liu, Bo Li, Kimberly Lu, and Dawn Xiaodong Song. Targeted backdoor attacks on deep learning systems using data poisoning. *ArXiv*, abs/1712.05526, 2017.

Siyuan Cheng, Yingqi Liu, Shiqing Ma, and Xiangyu Zhang. Deep feature space trojan attack of neural networks by controlled detoxification. *arXiv preprint arXiv:2012.11212*, 2020.

Corinna Cortes and Vladimir Vapnik. Support-vector networks. *Machine learning*, 20(3):273–297, 1995.

Khoa Doan, Yingjie Lao, and Ping Li. Backdoor attack with imperceptible input and latent modification. *Advances in Neural Information Processing Systems*, 34, 2021.

Min Du, Ruoxi Jia, and Dawn Song. Robust anomaly detection and backdoor attack detection via differential privacy. *arXiv preprint arXiv:1911.07116*, 2019.

Fastai. Fastai/imagenette: A smaller subset of 10 easily classified classes from imagenet, and a little more french, 2019. URL `https://github.com/fastai/imagenette`.

Robert Geirhos, Jörn-Henrik Jacobsen, Claudio Michaelis, Richard Zemel, Wieland Brendel, Matthias Bethge, and Felix A Wichmann. Shortcut learning in deep neural networks. *Nature Machine Intelligence*, 2(11):665–673, 2020.

Tianyu Gu, Brendan Dolan-Gavitt, and Siddharth Garg. Badnets: Identifying vulnerabilities in the machine learning model supply chain. *arXiv preprint arXiv:1708.06733*, 2017.

Jonathan Hayase, Weihao Kong, Raghav Somani, and Sewoong Oh. Spectre: defending against backdoor attacks using robust statistics. In Marina Meila and Tong Zhang (eds.), *Proceedings of the 38th International Conference on Machine Learning*, volume 139 of *Proceedings of Machine Learning Research*, pp. 4129–4139. PMLR, 18–24 Jul 2021. URL `https://proceedings.mlr.press/v139/hayase21a.html`.

Kaiming He, Xiangyu Zhang, Shaoqing Ren, and Jian Sun. Deep residual learning for image recognition. In *Proceedings of the IEEE conference on computer vision and pattern recognition*, pp. 770–778, 2016.

Kunzhe Huang, Yiming Li, Baoyuan Wu, Zhan Qin, and Kui Ren. Backdoor defense via decoupling the training process. In *International Conference on Learning Representations*, 2022.

Soheil Kolouri, Aniruddha Saha, Hamed Pirsiavash, and Heiko Hoffmann. Universal litmus patterns: Revealing backdoor attacks in cnns. In *Proceedings of the IEEE/CVF Conference on Computer Vision and Pattern Recognition*, pp. 301–310, 2020.

Alex Krizhevsky. Learning multiple layers of features from tiny images. *University of Toronto*, 05 2012.

Yige Li, Xixiang Lyu, Nodens Koren, Lingjuan Lyu, Bo Li, and Xingjun Ma. Anti-backdoor learning: Training clean models on poisoned data. *Advances in Neural Information Processing Systems*, 34, 2021a.

Yige Li, Xixiang Lyu, Nodens Koren, Lingjuan Lyu, Bo Li, and Xingjun Ma. Neural attention distillation: Erasing backdoor triggers from deep neural networks. *arXiv preprint arXiv:2101.05930*, 2021b.

Yiming Li, Yong Jiang, Zhifeng Li, and Shu-Tao Xia. Backdoor learning: A survey. *IEEE Transactions on Neural Networks and Learning Systems*, 2022.

Yuezun Li, Yiming Li, Baoyuan Wu, Longkang Li, Ran He, and Siwei Lyu. Invisible backdoor attack with sample-specific triggers. In *Proceedings of the IEEE/CVF International Conference on Computer Vision*, pp. 16463–16472, 2021c.

Yannan Liu, Lingxiao Wei, Bo Luo, and Qiang Xu. Fault injection attack on deep neural network. In *2017 IEEE/ACM International Conference on Computer-Aided Design (ICCAD)*, pp. 131–138. IEEE, 2017a.

Yunfei Liu, Xingjun Ma, James Bailey, and Feng Lu. Reflection backdoor: A natural backdoor attack on deep neural networks. In *European Conference on Computer Vision*, pp. 182–199. Springer, 2020.

Yuntao Liu, Yang Xie, and Ankur Srivastava. Neural trojans. In *2017 IEEE International Conference on Computer Design (ICCD)*, pp. 45–48. IEEE, 2017b.

Anh Nguyen and Anh Tran. Wanet–imperceptible warping-based backdoor attack. *arXiv preprint arXiv:2102.10369*, 2021.

Tuan Anh Nguyen and Anh Tran. Input-aware dynamic backdoor attack. *Advances in Neural Information Processing Systems*, 33:3454–3464, 2020.

Xiangyu Qi, Tinghao Xie, Ruizhe Pan, Jifeng Zhu, Yong Yang, and Kai Bu. Towards practical deployment-stage backdoor attack on deep neural networks. In *Proceedings of the IEEE/CVF Conference on Computer Vision and Pattern Recognition*, pp. 13347–13357, 2022.

Yankun Ren, Longfei Li, and Jun Zhou. Simtrojan: Stealthy backdoor attack. In *2021 IEEE International Conference on Image Processing (ICIP)*, pp. 819–823. IEEE, 2021.

Peter J Rousseeuw. Silhouettes: a graphical aid to the interpretation and validation of cluster analysis. *Journal of computational and applied mathematics*, 20:53–65, 1987.

Olga Russakovsky, Jia Deng, Hao Su, Jonathan Krause, Sanjeev Satheesh, Sean Ma, Zhiheng Huang, Andrej Karpathy, Aditya Khosla, Michael Bernstein, et al. Imagenet large scale visual recognition challenge. *International journal of computer vision*, 115(3):211–252, 2015.

Mark Sandler, Andrew Howard, Menglong Zhu, Andrey Zhmoginov, and Liang-Chieh Chen. Mobilenetv2: Inverted residuals and linear bottlenecks. In *Proceedings of the IEEE conference on computer vision and pattern recognition*, pp. 4510–4520, 2018.

Reza Shokri et al. Bypassing backdoor detection algorithms in deep learning. In *2020 IEEE European Symposium on Security and Privacy (EuroS&P)*, pp. 175–183. IEEE, 2020.

Karen Simonyan and Andrew Zisserman. Very deep convolutional networks for large-scale image recognition. *arXiv preprint arXiv:1409.1556*, 2014.

Johannes Stallkamp, Marc Schlipsing, Jan Salmen, and Christian Igel. Man vs. computer: Benchmarking machine learning algorithms for traffic sign recognition. *Neural networks*, 32:323–332, 2012.

Di Tang, XiaoFeng Wang, Haixu Tang, and Kehuan Zhang. Demon in the variant: Statistical analysis of dnns for robust backdoor contamination detection. In *30th {USENIX} Security Symposium ({USENIX} Security 21)*, 2021.

Brandon Tran, Jerry Li, and Aleksander Madry. Spectral signatures in backdoor attacks. *arXiv preprint arXiv:1811.00636*, 2018.

Alexander Turner, Dimitris Tsipras, and Aleksander Madry. Label-consistent backdoor attacks. *arXiv preprint arXiv:1912.02771*, 2019.

Laurens Van der Maaten and Geoffrey Hinton. Visualizing data using t-sne. *Journal of machine learning research*, 9(11), 2008.

Bolun Wang, Yuanshun Yao, Shawn Shan, Huiying Li, Bimal Viswanath, Haitao Zheng, and Ben Y Zhao. Neural cleanse: Identifying and mitigating backdoor attacks in neural networks. In *2019 IEEE Symposium on Security and Privacy (SP)*, pp. 707–723. IEEE, 2019.

Pengfei Xia, Hongjing Niu, Ziqiang Li, and Bin Li. A statistical difference reduction method for escaping backdoor detection. *arXiv preprint arXiv:2111.05077*, 2021.

Xiaojun Xu, Qi Wang, Huichen Li, Nikita Borisov, Carl A Gunter, and Bo Li. Detecting ai trojans using meta neural analysis. In *Proceedings of the IEEE Symposium on Security and Privacy (May 2021)*, 2021.

Nan Zhong, Zhenxing Qian, and Xinpeng Zhang. Imperceptible backdoor attack: From input space to feature representation. *arXiv preprint arXiv:2205.03190*, 2022.

(a) (b) (c) (d) (e) (f) (g)

(h) Adap-Blend (Test) & Blend (i) Adap-Blend (j) 1st Trigger (k) 2nd Trigger (l) 3rd Trigger (m) 4th Trigger (n) Adap-K (Test)

Figure 6: **Poison demonstration.**

A Experiment Configurations

A.1 Computational Environments

All of our experiments are conducted on a workstation with 48 Intel Xeon Silver 4214 CPU cores, 384 GB RAM, and 8 GeForce RTX 2080 Ti GPUs.

A.2 Attack Configurations

For each attack, we reuse the same triggers adopted in the paper. "Blend" and "Adap-Blend" use the blending-trigger (Fig 6a) with 20% opacity. "TaCT" uses the trojan square trigger (Fig6m) with 100% opacity. Eventually, "Adap-Patch" use the four triggers in Fig 6c-6f with 50%, 20%, 50% and 30% opacities, respectively. Specifically, each of their poison training sample randomly selects one of the four triggers (see Fig 6j-6m), while each test sample uses the enhanced two triggers demonstrated in Fig 6n.

The target class is set to class 0. 150 poison samples are used for "Blend", "BadNet", "ISSBA", "Dynamic" and "CL". For "TaCT", we use 150 poison samples and 150 cover samples. For "Adap-Blend", we use 150 payload samples and 150 regularization samples. For our "Adap-Patch", we use 150 payload samples and 300 regularization samples.

For all backdoor models, we adopt the standard training pipeline. SGD with a momentum of 0.9, a weight decay of 10^{-4}, and a batch size of 128, is used for optimization. Initially, we set the learning rate to 0.1. On CIFAR-10, we follow the standard 200 epochs stochastic gradient descent procedure, and the learning rate will be multiplied by a factor of 0.1 at the epochs of 100 and 150. On GTSRB we use 100 epochs of training, and the learning rate is multiplied by 0.1 at the epochs of 40 and 80.

We consider widely adopted data augmentations, i.e. `RandomHorizontalFlip` and `RandomCrop` for CIFAR-10 and `RandomRotation` for GTSRB. We notice that data augmentation may affect defense results significantly, while defenders do not know whether to use augmentation or not. Therefore, we report the better defense result of the two backdoor models with and without augmentation. In another sentence, we report **upper-bound results** of the defenses which might be affected by the incorporation of data augmentation during backdoor training. Also, to rule out the effect of randomness, we train three models on three seeds for each configuration, and report their average results.

A.3 Defense Configurations

- Spectral Signature Tran et al. (2018) removes $1.5 * \rho_p$ suspected samples from every class.
- Activation Clustering Chen et al. (2018) cleanses any clusters with size <35% of the class size.
- SCAn Tang et al. (2021) cleanses classes with scores larger than e.

Table 4: Results of our adaptive attacks on GTSRB.

Defenses→	No Defense		Spectral Signature		Activation Clustering		SCAn		SPECTRE	
Attacks ↓	ASR	CA	Elimination	Sacrifice	Elimination	Sacrifice	Elimination	Sacrifice	Elimination	Sacrifice
Blend	91.9	97.7	65.8	17.9	0.0	4.1	0.0	2.4	0.0	0.1
Adap-Blend	82.2	97.8	43.0	17.9	0.0	3.5	0.0	2.3	0.0	0.1
BadNet	99.5	97.8	100.0	25.2	97.7	2.3	99.2	0.5	100.0	0.3
Adap-Patch	63.1	97.8	74.4	25.4	0.0	0.3	35.6	4.6	0.0	0.1

- SPECTRE Hayase et al. (2021) removes $1.5 * \rho_p$ suspected samples only from the class with the highest QUE score.

B More Ablation Study

Since GTSRB and Imagenette contain different number of samples. For simplicity, we use the ratio of the whole training set to denote the number of poison samples, i.e. poison rate. We use ρ to denote the total ratio of poison samples. For our adaptive attacks, we use ρ_p to denote the ratio of payload poison samples and ρ_c to denote the ratio of regularization samples. Basically, $\rho = \rho_p + \rho_c$.

B.1 Adaptive Attacks on Different Datasets

In this subsection, we evaluate our attacks on different datasets. The same Resnet-20 architecture that we use in the main experiment is consistently used for all the experiments in this subsection.

B.1.1 GTSRB

GTSRB (Stallkamp et al., 2012) is a widely adopted dataset for backdoor study, for which we also evaluate our adaptive poisoning backdoor attacks on GTSRB.

Due to the imbalanced nature of GTSRB and the rotation-based data augmentation, we activate Adap-Patch with another set of inference-time asymmetric triggers, i.e. Fig 6d and Fig 6f, for high ASR. We use $\rho_p = 0.003$ and $\rho_c = 0.003$ for "Adap-Blend". We notice that "Adap-Patch" has a lower ASR on GTSRB than on CIFAR-10 (due to more classes); to boost up the ASR, we use $\rho_p = 0.005$ and $\rho_c = 0.01$ for "Adap-Patch". For comparison, we also show results of "Blend" ($\rho = 0.003$) and "BadNet" ($\rho = 0.005$).

As Table 4 tells, considerable amount of our adaptive poison samples could still survive the latent separability based defenses on GTSRB, as on CIFAR-10. Furthermore, compared with the non-adaptive attacks, our adaptive attacks consistently perform better (smaller elimination rates).

B.1.2 Imagenette

To illustrate the effectiveness adaptive strategy on high-resolution inputs (e.g., 224x224), we evaluate our adaptive poisoning backdoor attacks on a 10-classes Imagenet (Russakovsky et al., 2015) subset. Specifically, we take the commonly used Imagenette (Fastai, 2019) subset.

To successfully backdoor poison such a high-resolution dataset, selected triggers should usually be stronger (more evident visually). Specifically, for "Adap-Blend", we find the original blending trigger (Hellokitty) not strong enough, and replaced it with a random noise blending trigger (training poison alpha 0.15, test alpha 0.2; $\rho_p = 0.003, \rho_c = 0.003$); same trigger is used for "Blend" (alpha 0.2 all the time; $\rho_p = 0.003$). We also enhance "Adap-Patch" by training trigger opacities and their poison rates (Fig 6c-6d, opacity=1.0; $\rho_p = 0.01$, $\rho_c = 0.02$). For comparison, we use a stronger patch trigger ("Firefox", Fig6d) with $\rho_p = 0.01$ (the BadNet trigger is not strong enough for backdoor injection).

Table 5 shows that our adaptive attacks successfully circumvent the latent separability based defenses. On Imagenette, some defenses (Activation Clustering and SCAn with standard hyperparameters) are ineffective – they cannot cleanse any poison samples even for Blend and Firefox. Even so, we can still notice the superiority of our adaptive strategy over naive poisoning attacks (significantly smaller elimination rates against Spectral Signature and SPECTRE).

Table 5: Results of our adaptive attacks on Imagenette.

Defenses→	No Defense		Spectral Signature		Activation Clustering		SCAn		SPECTRE	
Attacks ↓	ASR	CA	Elimination	Sacrifice	Elimination	Sacrifice	Elimination	Sacrifice	Elimination	Sacrifice
Blend	93.1	90.1	21.4	4.4	0.0	3.2	0.0	0.0	100.0	0.1
Adap-Blend	60.8	89.7	7.1	4.4	0.0	3.1	0.0	0.0	0.0	0.4
Firefox	98.3	89.8	70.2	14.4	0.0	2.4	0.0	0.0	100.0	9.9
Adap-Patch	85.7	89.5	14.9	15.0	0.0	2.5	0.0	2.7	0.0	1.5

Table 6: Results of our adaptive attacks on other network architectures.

Defenses↓	**Archs→**	VGG-16		MobileNet-V2	
	Attacks→	Adap-Blend	Adap-Patch	Adap-Blend	Adap-Patch
Without Defense	ASR	74.0	63.6	72.2	96.4
	Clean Accuracy	93.4	93.6	92.2	92.3
Spectral Signature	Elimination Rate	59.3	53.3	3.3	2.7
	Sacrifice Rate	4.3	4.4	4.5	4.5
Activation Clustering	Elimination Rate	0.0	0.0	0.0	0.0
	Sacrifice Rate	0.0	0.0	0.0	0.0
SCAn	Elimination Rate	0.0	0.0	0.0	0.0
	Sacrifice Rate	0.0	0.0	0.0	4.7
SPECTRE	Elimination Rate	0.0	0.0	0.0	0.0
	Sacrifice Rate	0.5	0.5	0.5	0.5

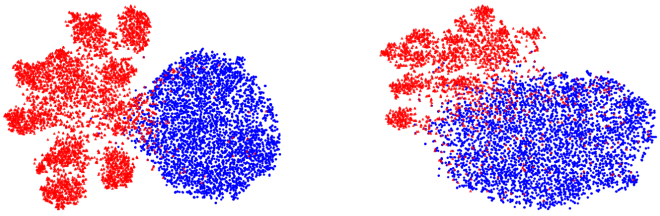

(a) WaNet (b) Refool

Figure 7: t-SNE Visualization of latent separability of WaNet and Refool on CIFAR-10.

B.2 Adaptive Attacks on Different Architectures

We also consider other model architectures, e.g., VGG-16 (Simonyan & Zisserman, 2014) and MobileNet-V2 (Sandler et al., 2018). We evaluate these architectures on CIFAR-10 against our adaptive attacks. Notice that these architectures have much larger latent spaces – MobileNet-V2 has a latent space of dimension 1280, and VGG-16 has a latent space of dimension 512 (for comparison, 64 for ResNet-20). Therefore, we have to adapt some defense configurations. Specifically, SCAn could not finish computing for MobileNet-V2 after 2h, so we manually reduce the latent representation's dimension to 128 by PCA before SCAn starts processing.

Overall, we show that our adaptive attacks also effectively circumvent latent separation based defenses. In Table 6, we demonstrate our adaptive attacks with these network architectures on CIFAR-10. As shown, none of these latent separability based defenses could completely eliminate our backdoor poison samples and most of them completely fail.

C Other State-of-the-art Backdoor Attacks

We also consider some other state-of-the-art backdoor attacks built on "advanced triggers". We illustrate that they also suffer from latent separation. We take Refool (Liu et al., 2020) and WaNet (Nguyen & Tran, 2021) as two examples. Refool constructs realistic reflection triggers for backdoor injection, while WaNet uses warp transformation for each image as the backdoor trigger. We launch these attacks in a poison-only manner, where they require much larger poison rates ($\rho = 0.1$) for WaNet, $\rho = 0.05$ for Refool) to inject backdoors with non-trivial ASR. Their T-SNE visualizations in Fig 7 clearly reveals the latent separation.